

Article

Correlation of Structure with Crystalline to Amorphous Phase Transitions of 1,3,6-Substituted Fulvene Derived Molecular Glasses

Loren C Brown, Andrew Peloquin, Nicholas P. Godman, Gary James Balaich, and Scott T Iacono

J. Org. Chem., **Just Accepted Manuscript** • DOI: 10.1021/acs.joc.0c01014 • Publication Date (Web): 13 Jul 2020

Downloaded from pubs.acs.org on July 13, 2020

Just Accepted

“Just Accepted” manuscripts have been peer-reviewed and accepted for publication. They are posted online prior to technical editing, formatting for publication and author proofing. The American Chemical Society provides “Just Accepted” as a service to the research community to expedite the dissemination of scientific material as soon as possible after acceptance. “Just Accepted” manuscripts appear in full in PDF format accompanied by an HTML abstract. “Just Accepted” manuscripts have been fully peer reviewed, but should not be considered the official version of record. They are citable by the Digital Object Identifier (DOI®). “Just Accepted” is an optional service offered to authors. Therefore, the “Just Accepted” Web site may not include all articles that will be published in the journal. After a manuscript is technically edited and formatted, it will be removed from the “Just Accepted” Web site and published as an ASAP article. Note that technical editing may introduce minor changes to the manuscript text and/or graphics which could affect content, and all legal disclaimers and ethical guidelines that apply to the journal pertain. ACS cannot be held responsible for errors or consequences arising from the use of information contained in these “Just Accepted” manuscripts.

1
2
3
4
5
6
7
8

Correlation of Structure with Crystalline to Amorphous Phase Transitions of 1,3,6-Substituted Fulvene Derived Molecular Glasses

9 Loren C. Brown, Andrew J. Peloquin, Nicholas P. Godman,^b
10 Gary J. Balaich,* Scott T. Iacono*

11
12
13
14
15
16
17
18
19

^aDepartment of Chemistry & Chemistry Research Center, Laboratories for Advanced
Materials, United States Air Force Academy, Colorado Springs, Colorado (USA)

^bAir Force Research Laboratory, Materials and Manufacturing Directorate,
Wright-Patterson Air Force Base, Dayton, Ohio (USA)

*Correspondence e-mail: gary.balaich@usafa.edu or scott.iacono@usafa.edu

20
21
22
23

Abstract:

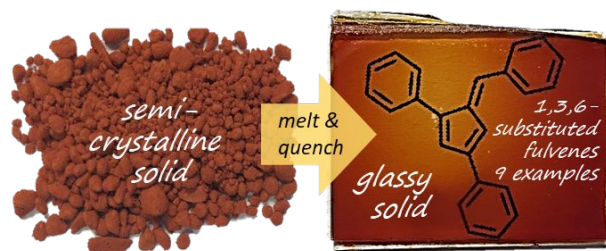
24
25
26
27
28
29
30
31
32
33
34
35
36
37
38
39
40
41

An investigation into the crystalline to amorphous phase transitions of prepared 1,3,6-substituted pentafulvenes showed the expected reversible heated melt and cooling recrystallization in only a few examples. Systematic incorporation of bulky substituents at the 6-position of the fulvene ring led to non-reversible thermal behavior, rendering phases that were locked into glassy, vitrified states. These molecular glasses produced physically translucent and amorphous features with glass transition temperatures in the range of 61–77 °C, comparable with high-strength plastics such as polyethylene terephthalate. Additionally, the melting point transitions and the resulting heat of fusion values were found to be directly influenced by the nature of the 6-position substituent. Single crystal X-ray crystallography showed that in some cases fulvenes possessing fused aromatics exhibited a high degree of intermolecular π - π stacking. These results point to a class of molecular glass formers as host materials possessing tunable bulk properties for potentially new optical applications.

42
43
44
45
46
47
48
49
50
51
52
53
54
55
56
57
58
59
60

Keywords: Fulvene; Crystallinity; Amorphous; Vitrogen; Molecular Glass; Calorimetry

TOC Graphic:



Molecular Pentafulvene Glasses – Melt conversion of crystalline 1,3,6-substituted fulvenes to a locked, vitreous state affords new translucent, colored amorphous materials. The crystalline and amorphous properties are correlated with their structure using single crystal X-ray diffraction and calorimetric techniques.

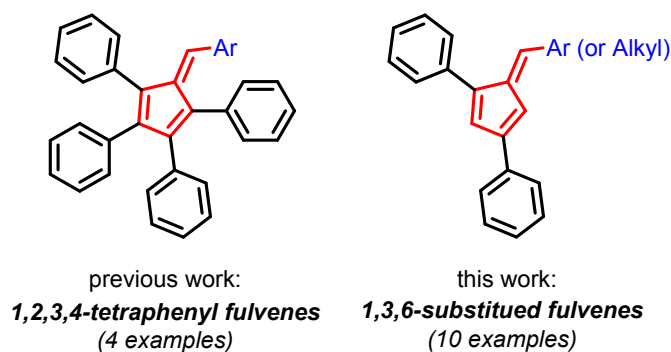
Introduction

Small molecule crystallization is driven by intermolecular forces, a process that is well understood and generally accepted as reversible upon additional heating and cooling cycles. However, a phenomenon that is less understood occurs when low molecular weight compounds fail to crystallize under conditions below those known for their thermodynamic solid state phase changes.^{1,2} Although 1,3,6-triaryl substituted fulvenes (Figure 1) undergo crystalline melt transitions, to our surprise, this was followed by the formation of amorphous glassy states which could be validated on visual inspection as well as by calorimetric measurements. Such a process is caused by vitrification, a phenomenon that allows low molecular weight molecules to become structurally interlocked in random configurations by overcoming intermolecular forces that would normally induce crystallization. The requirements for small molecules to possess glass-forming properties include a combination of large molecular weight, the presence of

1
2
3
4 aromatic rings, molecular asymmetry, a large number of rotatable bonds, branched
5 carbon skeletons, and/or a combination of electronegative atoms.³⁻⁶ Vitrification is
6
7 common in high molecular weight, chain-extended linear or network architectures such
8
9 as oligomers or polymers and quantified by the glass transition temperature (T_g).
10
11 However, rheological studies on super-cooled small molecule liquids such as glycerol and
12
13 *ortho*-terphenyl indicate that long range order of these molecules can also be achieved in
14
15 the glassy state.⁷ Further, in a recent comprehensive study of industrially important
16
17 compounds, small molecules of the phenyl propanol family such as 1-phenyl-1-propanol,
18
19 glycerol, and 2-isopropylphenol were found to exhibit T_g 's slightly below or above room
20
21 temperature at standard atmospheric pressure.⁸ However, since the introduction of
22
23 organic monomeric glasses by Molaire and Johnson⁹, molecules that exhibit a T_g above
24
25 room temperature have been reported only in narrow fields of interest and likely
26
27 overlooked for their promising applications. For example, amorphous solid dispersions
28
29 (ASD), drug formulations composed of active pharmaceutical ingredients (API's) dispersed
30
31 in an amorphous glassy matrix, have been shown to improve important variables of
32
33 biological drug efficacy such as transport and dissolution.⁹⁻¹⁴ The value of the glassy state
34
35 has also been exploited for incorporating liquid crystal mesogens into low molecular
36
37 weight matrices for information storage materials.¹⁵ Randomly organized, glassy
38
39 materials have also been used as host matrices to lock in chromophore guests in the
40
41 design of optoelectronic materials.¹⁶⁻¹⁸ More recently, small molecules have been
42
43 designed for well-defined fluorescent glasses,¹⁹ non-linear optics,²⁰ charge transporting
44
45
46
47
48
49
50
51
52
53
54
55
56
57
58
59
60

1
2
3
4
5 devices,²¹ and radioluminescence.²² Related to fulvenes of interest to this work, it has
6
7 been reported that 1,2,3,4-tetraphenyl substituted fulvenes exhibited T_g 's of over 100 °C,
8
9 and correlate with the nature of the 6-substituent (Figure 1).²³⁻²⁵

10
11
12 To our knowledge, there have been no systematic thermal studies of substituted
13
14 fulvenes that involve structural correlations between crystallinity and their amorphous
15
16 nature. Motivated by this lapse, it is the purpose of this work to present a study of the
17
18 melting phase transitions of 1,3,6-substituted fulvenes as a function of the 6-substituent
19
20 on the fulvene core as supported by DSC and single crystal X-ray diffraction. The
21
22 amorphous nature of 1,3,6-substituted fulvenes that can achieve a vitrified state was
23
24 studied, and their corresponding T_g values were correlated to the nature of the
25
26 substituent at the 6-position. Insight gained from this study expands the application of
27
28 these fulvenes as low molecular weight glass formers for a new class of amorphous host
29
30 matrix materials, obtainable from operationally simple and high yielding synthetic
31
32 procedures.
33
34
35
36
37



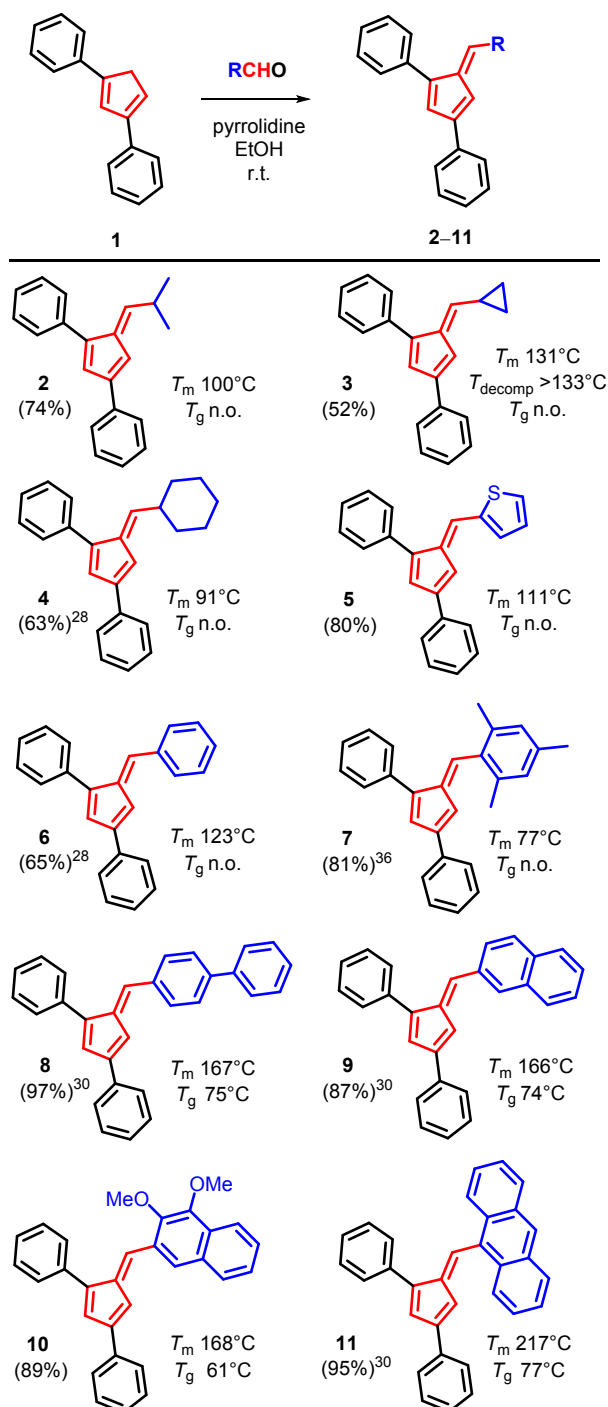
51
52
53
54
55
56
57
58
59
60

Figure 1. Generic structural depiction of fulvenes: previously reported work²⁴⁻²⁶ compared with the present investigation.

Results and Discussion

Fulvene Synthesis

The synthesis of 1,3,6-substituted fulvenes **2–11** was carried out by the coupling of 1,3-diphenylcyclopentadiene **1** with the corresponding substituted aldehydes in pyrrolidine-promoted ethanolic media according to a modified literature procedure (Scheme 1).²⁶ Good overall isolated yields (52–97%) of high purity 1,3,6-substituted fulvenes **2–11** were afforded as microcrystalline solids of varying color depending on the nature of the 6-position, several of which were previously reported for their optical^{27,28} as well as electrochemical²⁹ properties. For the purposes of this study, selected 6-substituted fulvenes were chosen and are grouped according to branched and cyclic aliphatic (**2–4**), functionalized aromatic (**5–8**), and fused aromatic of varying architecture (**9–11**).



49
50
51
52
53
54
55
56
57
58
59
60

Scheme 1. Synthesis of 1,3,6-substituted fulvenes (2-11) from 1,3-diphenylcyclopentadiene (2) and their corresponding isolated yield (%), melting point (T_m), and glass transition temperature (T_g) as observed by DSC (second scan).

Crystalline Properties

The melting point (T_m) and enthalpy of fusion (ΔH_f) values for fulvene compounds **2–11** are plotted in Figure 2. There are distinct differences in both T_m and ΔH_f that depend on the nature of the substitution at the 6-position (Figure 2). Aliphatic fulvenes **2** and **3** and aromatic fulvene compounds **5** and **6** have melting points above 100 °C, narrowly ranging between 100–131 °C with the highest melting 6-aliphatic substituted fulvene being the cyclopropyl-functionalized **3**. Fulvenes **4** and **7** fall significantly below the observed mp trend (91 °C (**4**) and 77 °C (**7**)). This is presumably due to the highly flexible nature of the cyclohexyl functionalized fulvene **4** and the bulky nature of the 2,4,6-trimethylphenyl substituted fulvene **7**, each structure causing disruptions of the predominating van der Waals interactions in the solid state. The perturbation of the intermolecular forces is further validated given the lower ΔH_f observed for **4** (53 J/g) and **7** (57 J/g), compared to the series of all other fulvenes studied wherein the ΔH_f values fall in the narrow range of 95–109 J/g. Interestingly, as bulky aromatic groups are substituted (fulvenes **8–11**), there is a significant melting point increase from fulvene **3**. While the biphenyl- **8**, naphthyl- **9**, and 2,3-dimethoxynaphthyl- **10** substituted fulvenes were observed to have similar melt transitions (166–168 °C), the anthracene analogue **11** produced the highest T_m (217 °C) which is 49–51 °C higher among this series. The large increase in melting point for fulvene **11** appears to be a direct result of observed π – π stacking induced by the anthracene units (vide infra, Figure 4). Curiously, fulvene **8** was observed to have distinct, but overlapping melting points at 167.3 and 167.9 °C, likely due to two polymorphs generated by the

rotational motion of the biphenyl unit at the 6-position.

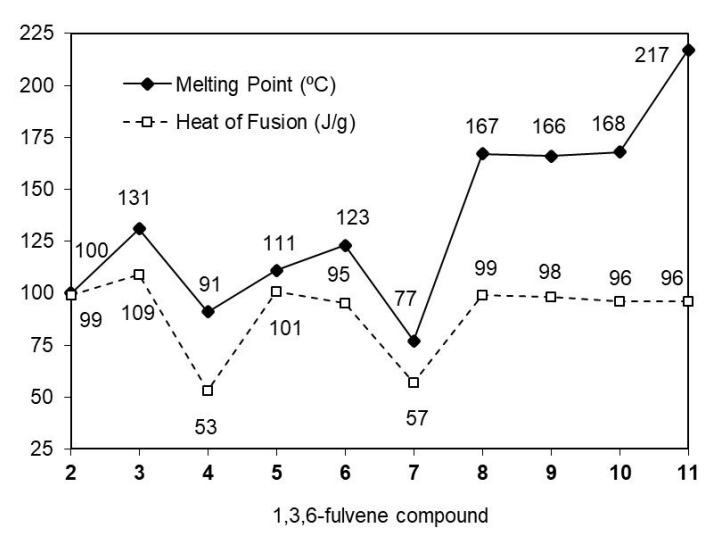


Figure 2. DSC derived melting points and heat of fusion data for fulvene compounds **2–11**.

In the crystal structures of fulvenes **2**, **8** and **11**, some correlation of crystal packing to observed thermal behavior could be made. Single crystal X-ray structures for fulvenes **4** and **6** (Scheme 1) were previously reported,²⁸ and the structures for fulvenes **2**, **8** and **11** are included and discussed as part of this work. Each fulvene molecular structure exhibited the expected alternating short-long bond distances within the fulvene ring, and the exocyclic bond distances and angles were found to be consistent with those obtained from similar 1,3-diphenyl-6-substituted structures.²⁸ The correlation between the crystal structures and their respective melts lies within the type of intermolecular forces at play and the contact area over which these forces act. In this study the data (vide infra) demonstrate that the size, shape and type of the 6-position substituent of the fulvene can have significant effects in a correlation comparing aliphatic to linked aromatic and fused

1
2
3
4 aromatic groups at the 6-position of 1,3-diphenylfulvenes. In particular, there is an
5 approximately linear increase in mp from fulvene **2** to **8** to **11** (Figure 2), and this trend is
6 herein related to crystal packing effects in the solid state structures of these fulvenes.
7
8
9

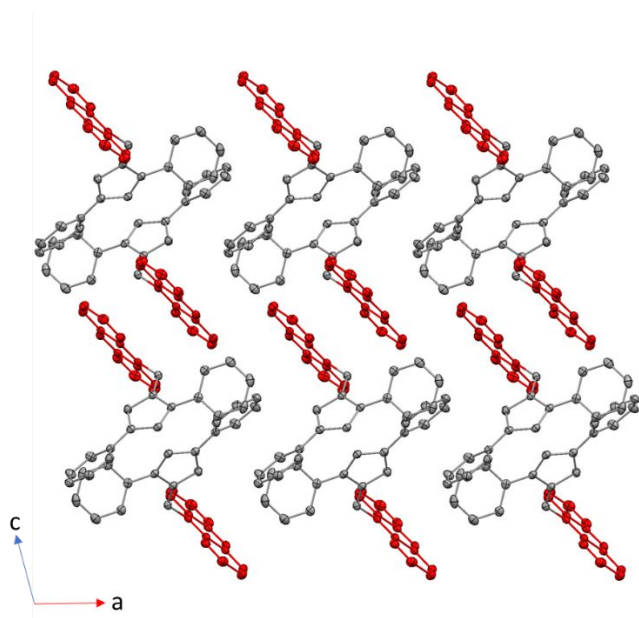
10
11
12 Molecules of the 6-isopropyl fulvene **2** pack in a zig-zag pattern along the c-direction
13 with weak van der Waals contacts between 6-ⁱPr and 1-Ph substituents (H, head) that
14 orient head-to-head (H-H) and weak π - π interactions of the 3-Ph rings (T, tail) that orient
15 tail-to-tail (T-T) (Figure S1). The 3-Ph ring slipped π - π stacking (distance between mean
16 planes of 3-Ph rings, 3.377 Å, Figure S2) orients fulvene molecules in a T-T fashion in the
17 middle of columns that run perpendicular to the c-direction. Adjacent columns that are
18 separated along the c-direction interact via the H-H interactions, producing a repeating
19 zig-zag H-T-T-H packing sequence (Figure S1). Although the intermolecular forces holding
20 crystals of fulvene **2** are overcome at the mp of 100° C, the mp's of fulvenes **4** (91° C) and
21 **7** (77° C) are significantly lower (Scheme 1), producing a break in the mp trend between
22 fulvenes **2** and **8**. The crystal structures of fulvenes **4**²⁸ and **7**³⁶ indicate that very weak
23 intermolecular interactions of the C-H--- π type dominate. In addition, we believe that
24 the conformational flexibility of the 6-cyclohexyl group (**4**) and the shape of the larger 6-
25 mesityl group (**7**) disrupt stronger intermolecular forces and result in significantly lower
26 mp's for these fulvenes.
27
28
29
30
31
32
33
34
35
36
37
38
39
40
41
42
43
44
45
46
47
48

49 In contrast, the extended shape and rigidity of the 6-biphenyl substituent of fulvene
50 **8** contributes to a significantly higher mp (167° C). In the crystal structure of the 6-
51 biphenyl fulvene **8**, the biphenyl groups participate in an interleaved packing along the c-
52
53
54
55
56
57
58
59
60

1
2
3
4 direction, with the long axes of the biphenyl groups (H, head) oriented H-H and
5
6 maximizing van der Waals contacts in the space between the 6-biphenyl and 3-Ph
7
8 substituents on adjacent fulvene rings (Figure S3). This packing arrangement leaves the
9
10 1,3-diphenylfulvene rings (T, tail) oriented T-T and the entire structure devoid of any π - π
11
12 stacking between phenyl or biphenyl groups on adjacent fulvene units. Each biphenyl
13
14 group has 6 nearest neighbor biphenyl groups that are distributed in layers that run along
15
16 the c-direction and that bisect the b-direction. Although there are no π - π stacking
17
18 interactions in the 6-biphenyl fulvene solid state structure, the energy required to disrupt
19
20 this packing and to reach the melting point transition is higher compared to the 6-
21
22 isopropyl fulvene and provides one of the higher mp values in this series of fulvenes
23
24 (Figure 2). We correlate this difference mainly to the effect of the long biphenyl group at
25
26 the 6-position with its resulting significantly larger van der Waals contact area.
27
28
29
30
31
32
33

34 The structure of fulvene **11** illustrates how the van der Waals contact area can be
35
36 maximized by extended and fused ring aromatics that drive intermolecular π - π stacking
37
38 at the 6-position of 1,3-diphenylfulvenes.²⁸ A view down the b-axis in the structure of
39
40 fulvene **11** reveals chains of fulvene molecules running along the c-direction with an H-H
41
42 (6-anthracene rings) and a T-T (1,3-diphenylfulvene rings) orientation and linked via a
43
44 slipped π - π stacking of the 6-anthracene rings (Figure 3, 4). Although the 6-anthracene
45
46 ring planes on adjacent fulvene molecules are oriented parallel to each other, the 1-Ph
47
48 and 3-Ph rings from adjacent molecules are positioned nearly perpendicular to each other
49
50 running along the b-direction and nearly perpendicular to the 6-anthracene rings of
51
52
53
54
55
56
57
58
59
60

1
2
3
4
5 fulvene molecules in separate chains. This packing gives rise to a herringbone pattern in
6
7 the ac plane, maximizing slipped π - π overlap of the larger 6-anthracene units (distance
8
9 between mean planes of 6-anthracene rings, 3.491 Å, Figure 4) as well as C-H \cdots π
10
11 interactions of the 1-Ph and 3-Ph rings with each other and with nearest neighbor
12
13 anthracene units. The larger ring tilt angle for the plane of the 3-Ph ring from the fulvene
14
15 ring plane ($30.38(4)^\circ$) as well as the very large ring tilt angle of the plane of the 6-
16
17 anthracene units from the fulvene plane ($80.51(4)^\circ$) are probably due to the significant
18
19 effect of this crystal packing on the molecular structure of **11** in the solid state. This solid
20
21 state structure gives rise to the highest observed melting point (217°C) in the series of
22
23 fulvenes highlighted in this paper.
24
25
26
27
28
29



50
51 **Figure 3.** Packing view of **11** showing 6-anthracene
52 ring π - π interactions. Thermal ellipsoids shown at
53 50%. Hydrogen atoms were omitted for clarity.
54
55
56
57

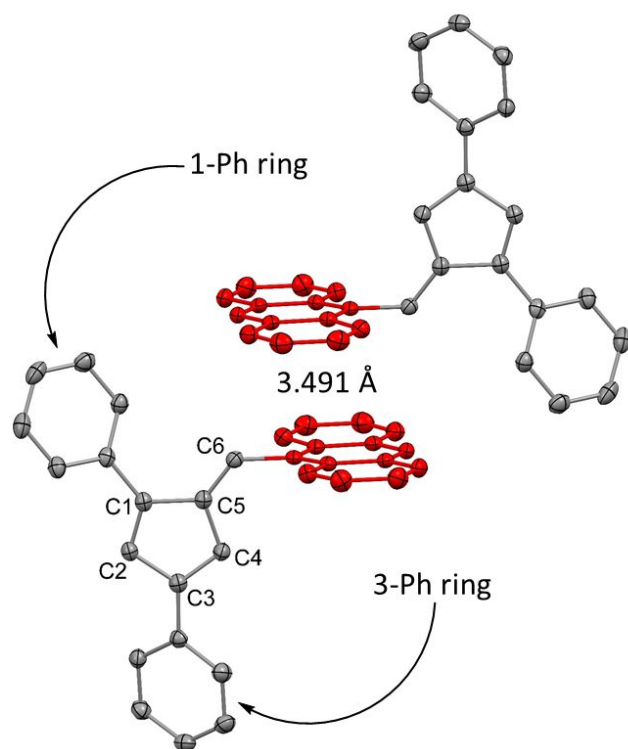


Figure 4. Thermal ellipsoid view of **11** depicting π - π overlap between adjacent molecules (distance shown is separation of 6-anthracene ring mean planes). Thermal ellipsoids shown at 50%. Hydrogen atoms were omitted for clarity.

Amorphous Properties

The amorphous thermal properties of fulvenes **2–11** were investigated utilizing DSC, and the results varied significantly depending on the nature of the substituent at the 6-position. Initial study of the aliphatic series beginning with isopropyl fulvene **2** showed typical behavior of a microcrystalline solid by revealing a T_m at 100 °C and, upon cooling, a late developing crystallization temperature (T_c) at 50 °C. Partial vitrification of **2** was shown by the observed suppression of the exothermic heat of crystallization (ΔH_c from -43 J/g to -11 J/g) after only one additional heating/cooling cycle (Figure 5). Upon the third

1
2
3
4 heating/cooling cycle, no T_g or T_c was evident, indicating that fulvene **2** was transformed
5
6 into an entirely amorphous phase. Observation of the pellet in the DSC pan after these
7
8 thermal cycles showed a translucent glass-like coating with poor mechanical properties.
9
10 For comparison, cyclopropyl fulvene **3** could not be converted to a glass state by thermal
11
12 annealing of the solid sample. Fulvene **3** gave a sharp melt transition at 131 °C, but was
13
14 immediately followed by an exothermic event (onset at 131 °C) affording a dark brown
15
16 solid. In the ^1H NMR (CDCl_3) spectrum of the brown solid, indeterminable peaks were
17
18 observed, presumably due to oligomerized products from ring opening of the cyclopropyl
19
20 ring. The obvious target for comparison in the thermal analysis of the aliphatic series is
21
22 the 6-cyclopentyl fulvene. However, attempts to prepare cyclopentyl fulvene **12a**
23
24 (Scheme 2) using the same synthetic procedure for fulvenes **2–11** did not afford the
25
26 desired fulvene product. Instead, a [1,7]-hydride shift from fulvene **12a** resulted in the
27
28 formation of the cyclopentadiene isomer **12b** as the preferred product (Scheme 2).
29
30 Computational work has shown that similar [1,7]-hydride shifts occur for 6,6-
31
32 dimethylfulvene either by a unimolecular or bimolecular process both having the same
33
34 activation energies.³¹ X-ray crystallographic analysis showed a pattern in bond lengths
35
36 for the cyclopentadiene ring and exocyclic C-C bonds consistent with the structure of **12b**
37
38 (Figure S6, 1.467(2), C5-C6 long bond; 1.342(2), C6-C19 short bond). A singlet peak at δ
39
40 3.82 in the ^1H NMR spectrum pointed to the cyclopentadiene ring CH_2 further confirming
41
42 the isolated structure of **12b**.
43
44
45
46
47
48
49
50
51
52
53
54
55
56
57
58
59
60

Although not a fulvene, the thermal analysis of **12b** proved insightful. The cyclopentadiene adduct **12b** produced a reversible T_m (145 °C) and T_c (87 °C) after repeated heating-cooling cycles as shown in Figure 5. This reflects the structural rigidity of 1,3,6-substituted fulvenes compared with **12b**. By shifting the exocyclic double bond from C5–C6 in a fulvene to C6–C19 in **12b**, this double bond is no longer constrained to the same plane as the cyclopentadiene system. By allowing rotation around the C5–C6 bond, extended π conjugation is disturbed, decreasing the potential for the long-range order necessary for formation of a glassy state, and this results in reversible T_m and T_c values.

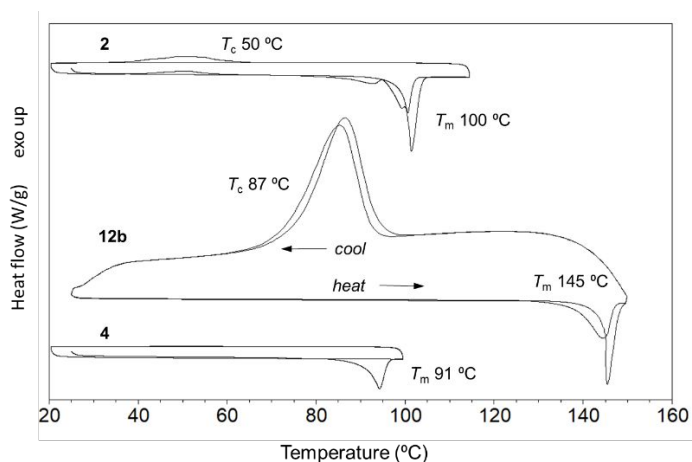
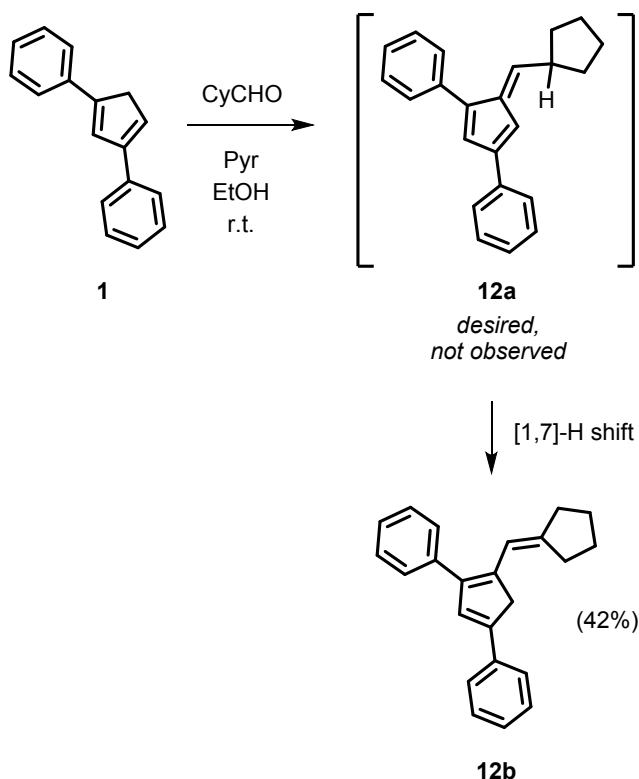


Figure 5. First and second DSC cycles for fulvenes **2** and **4** (top and bottom thermograms) and cyclopentadiene **12b** (middle thermogram).

DSC analysis of the cyclohexyl functionalized fulvene **4** revealed that an entirely vitrified, glassy state could be achieved by a single heating cycle past the melting transition ($T_m = 91$ °C). There was no evidence of recrystallization during the cooling part

1
2
3
4
5 of the first cycle, and upon further heating after the second cycle, there was no observed
6
7 melting transition. This behavior was driven by the increased entanglement of the
8
9 cyclohexyl rings in the 6-position of the fulvene. Inspection of the DSC pan revealed a
10
11 translucent dark orange and brittle solid circular disk that could be re-dissolved in
12
13 common organic solvents, further validating the glassy state achieved by this fulvene.
14
15 NMR and GC-MS analysis of this formed fulvene glass showed no indication of
16
17 degradation. However, the cyclohexyl ring, which is capable of adopting multiple
18
19 conformers in the solid state, did not sufficiently induce long-range order, resulting in a
20
21 non-observable glass transition temperature (T_g) even after the third heating scan.
22
23 Furthermore, fulvenes substituted with thiophene **5**, phenyl **6**, and mesityl **7** also do not
24
25 exhibit a T_g after reaching their melting points.
26
27
28
29
30
31
32
33
34
35
36
37
38
39
40
41
42
43
44
45
46
47
48
49
50
51
52
53
54
55
56
57
58
59
60



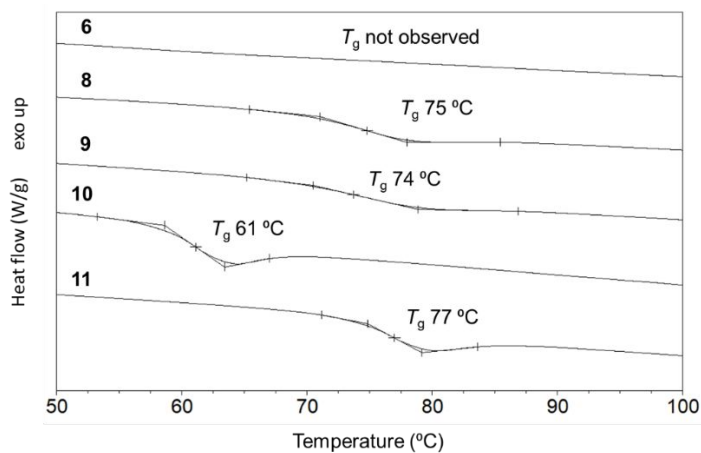
30
31
32
33
34

Scheme 2. Isomerization of fulvene **12a** – cyclopentadiene **12b** via a [1,7]-hydride shift.

35
36
37
38
39
40
41
42
43
44
45
46
47
48
49
50
51
52
53
54
55
56
57
58
59
60

In the DSC study of fulvenes with linked or fused ring aromatic substituents at the 6-position (**8-11**), well defined glass transition events were observed (Figure 6). Comparison of the DSC scan for the biphenyl fulvene **8** with the phenyl fulvene **6** showed a well-defined glass transition event at 75 °C, which was observed upon heating after one heat-melt-cool cycle. Additionally, the naphthyl **9** and anthracene **11** substituted fulvenes had similar T_g 's at 74 °C and 77 °C, respectively. Although not entirely anomalous, the 2,3-dimethoxynaphthyl fulvene **10** produced a slightly lower T_g (61 °C), but this was expected due to the freely rotating methoxy groups. Similar phenomena were observed with

1
2
3
4
5 1,2,3,4-substituted fulvenes (Figure 1), whereby the same correlation of an increase in T_g
6
7 was observed with bulkier functional groups at the 6-position.²⁴⁻²⁶
8
9



12
13
14
15
16
17
18
19
20
21
22
23
24
25
26
27
28 **Figure 6.** DSC trace of second scan immediately after
29 each fulvene melting point, showing selected T_g
30 values for fulvenes **6** and **8–11**.
31

32
33 In the DSC thermograms of fulvenes **2** and **4–7**, exotherms were observed when
34 heated beyond their melting transitions, and very broad T_g 's (60–70 °C) were observed
35 upon reheating. Fulvene **6** served as a model substrate to demonstrate this
36 phenomenon. As depicted in Figure 7, an initial heating to 200 °C produced a broad
37 exothermic event ($T_{max} = 163$ °C, $\Delta H = -29$ J/g). The second re-heating showed a slight
38 inflection in the thermogram (Figure 7, broad T_g) indicative of a developing glass
39 transition, but the fulvene exists in an entirely amorphous state. Additional heating to
40 200 °C and holding at this temperature for 5 h induced the formation of a defined T_g at
41 90 °C (Figure 7).
42
43
44
45
46
47
48
49
50
51
52
53
54
55
56
57
58
59
60

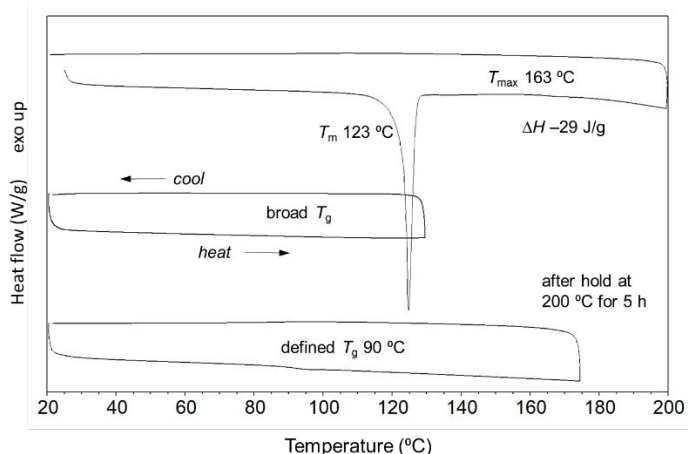
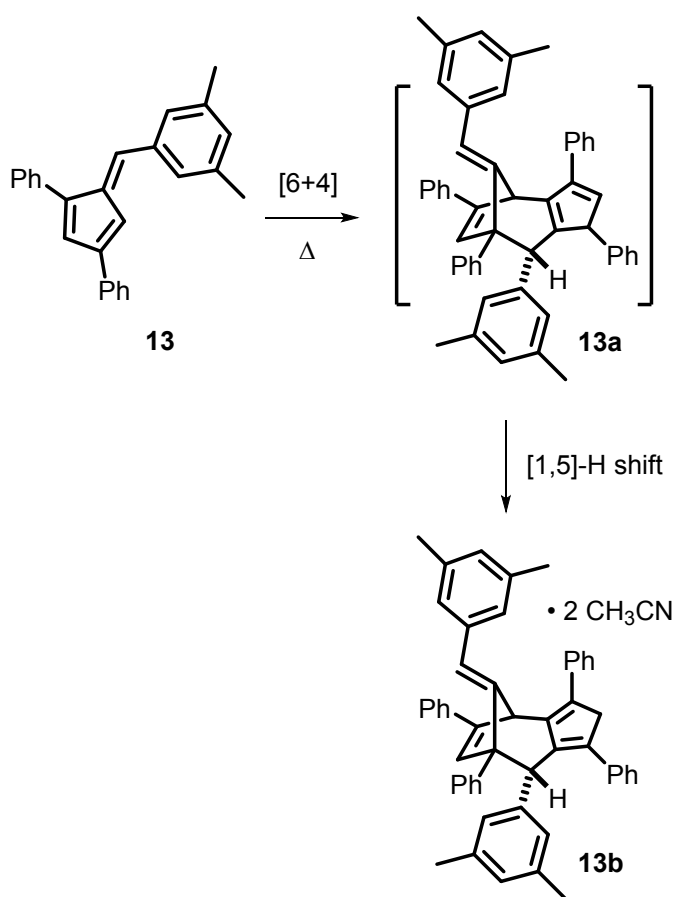


Figure 7. DSC thermogram overlay of fulvene **6**: initial melting and broad exotherm to 200 °C (top), second cooling and re-heating displaying a broad T_g (middle), and thermogram with defined T_g after 5h isothermal hold at 200 °C (bottom).

The observed development of a glass transition temperature upon thermal cycling of fulvenes **2** and **4-7** at 200 °C promoted further investigation. A [6 + 4] cycloaddition to afford dimerized adducts is consistent with the development of these defined T_g values and is further validated by results previously published.^{30,31} For example, cyclodimerization of phenyl fulvene **6** affords twice the molecular weight increase of 612.82 g/mol, a value in the range for which glass transition temperatures are expected for small molecules. These ideas are supported by the reported crystal structure of the 6-(3,5-dimethylphenyl) substituted fulvene dimer **13b** as shown in Scheme 3 (X-ray structure in Figure S7).³² Given the published experimental conditions by which **13b** was formed, we postulate the dimerization occurs via a [6 + 4] cycloaddition of **13**, with the initial formation of bicyclic **13a** followed by a [1,5]-hydride shift to the most stable adduct

1
2
3
4
5 **13b**. Also relevant to this cyclodimerization is the observation of intractable networks that
6
7 were obtained from the thermal heating of a 6-(3-styryl) fulvene at 125 °C. The
8
9 installation of the styryl moiety at the 6-position induced simultaneous vinyl-vinyl [2 + 2]
10
11 as well as vinyl-fulvene [2 + 4] cyclodimerizations, the former [2 + 2] being preferred based
12
13 on significant crystalline organization and the ability to obtain free spatial orientation in
14
15 the solid state.²⁸
16
17
18



48 **Scheme 3.** Thermally promoted [6+4]
49 cyclodimerization of fulvene **13** followed by
50 isomerization to the most stable adduct **13b**.
51 Thermal ellipsoids are shown at the 50% probability
52 level.
53
54
55
56
57

Conclusion

In this work, we carried out a systematic study relating crystalline to amorphous phase transitions of a series of 1,3,6-substituted fulvenes with varying degree of substitution at the 6-position. Similar ΔH_f data for these fulvenes suggest that analogous intermolecular forces predominate the melt transition, while data from single crystal X-ray diffraction demonstrated that fulvenes with linked or fused aromatic groups exhibited significantly higher melting points due to higher van der Waals contact areas and π - π stacking effects. We have also shown that the vitrified state could easily be achieved upon substitution with a cyclohexyl group at the 6-position, and that substitution at the 6 position with bulkier aromatic groups produced glassy materials with more well defined T_g values.

This work expands the previous scope of applicability of highly colored 1,3-diphenyl-6-substituted fulvenes²⁸ to fulvenes with application as precursors for the formation of glassy materials having tunable solid state optical properties. In the consideration of composite systems with other organic or inorganic fillers of interest, it is possible to blend various 6-substituted fulvenes in order to adjust their spectral absorbance properties as well as potentially tuning the T_g . Additionally, the synthesis of 1,3-diphenylcyclopentadiene compounds possessing reactive bromine functionalities³⁵ offers the ability to prepare a diverse pool of 1,3,6-substituted fulvene substrates that would further alter bulk physical properties of interest for molecular glasses. Finally, consideration of chain extended systems brings the opportunity to significantly influence solid state and solution state polymer architecture and microstructure by studying the

1
2
3
4 influence of the 1,3-diphenyl-6-substituted fulvenes or related 1,3,6-substituted fulvene
5
6 repeat units in the main chain.
7
8

9 **Experimental Section**

10 *General Methods*

11
12
13
14 Synthesis of 1,3-diphenylcyclopentadiene **1** was carried out using a previously
15
16 published procedure.²⁷ All solvents were purchased from commercial suppliers and used as
17
18 received unless otherwise noted. Syntheses of **2**, **3**, **5**, and **10** using **1** as the cyclopentadiene
19
20 starting material were carried out using a modified literature procedure as detailed
21
22 below.²⁸ The synthesis of fulvenes **4**, **6–9**, **11**, **13**, and fulvene dimer **13b** were previously
23
24 reported and successfully reproduced as necessary for this study.^{27,29,32,33}
25
26
27

28 *Instrumentation*

29
30
31 ¹H and ¹³C NMR data were obtained from a JEOL 500 MHz NMR spectrometer under
32
33 ambient temperature conditions and chemical shifts reported in parts per million (δ ppm).
34
35 Chemical shifts were referenced using the peak for residual CHCl₃ (δ 7.25) or TMS (δ 0.00)
36
37 for ¹H NMR and the peak for CDCl₃ (δ 77.0) for ¹³C NMR. Coupling constants for all spectra
38
39 are reported in Hertz (Hz).
40
41
42

43
44 Differential scanning calorimetry (DSC) analyses were performed on a TA Instruments
45
46 Q20 instrument utilizing aluminum hermetic pans. The analyses were carried out using a
47
48 5°C/min temperature gradient from 20 °C to 100-150 °C (for **2–7** and **12**) or to 250 °C (for
49
50 **8–11**), cooled to 20 °C under nitrogen, and repeated two additional times for three overall
51
52 scans. HRMS data of purified samples was obtained using a Synapt G2 HDMS time-of-
53
54
55
56
57
58
59
60

1
2
3
4
5 flight (MALDI-TOF) mass spectrometer located at the Central Analytical Mass
6
7 Spectrometry Facility at the University of Colorado at Boulder. Crystals of fulvenes **2**, **8**,
8
9 **11**, and cyclopentadiene **12b** were mounted on CryoLoops with Paratone oil, and data
10
11 collected at 100 K on a Bruker SMART APEX II CCD diffractometer equipped with Cu K_α
12
13 radiation (λ = 1.54178)
14
15

16
17 *1,3-diphenyl-6-(isopropyl)fulvene 2*
18

19 To a vigorously stirred mixture of 1,3-diphenylcyclopentadiene (3.07 g, 14.1 mmol) in
20
21 absolute EtOH (30 mL) under N₂ was added isobutyraldehyde (1.22 g, 16.9 mmol) and
22
23 pyrrolidine (1.50 g, 21.1 mmol), and the reaction mixture maintained at room
24
25 temperature for 24 hrs. The orange precipitate from the reaction mixture was vacuum
26
27 filtered, washed with cold absolute EtOH (3 × 10 mL), and vacuum dried to give **2** as a
28
29 bright orange, microcrystalline solid (2.84 g, 74%). Crystals suitable for single crystal X-ray
30
31 diffraction were obtained from petroleum ether by slow evaporation. ¹H NMR (500 MHz,
32
33 CDCl₃) 7.69 – 7.24 (m, 10H), 6.94 (s, 1H), 6.86 (s, 1H), 6.33 (d, 1H, J = 10.0 Hz), 3.15 (m,
34
35 1H), 1.17 (d, 6H, J = 6.7 Hz). ¹³C NMR (125 MHz, CDCl₃) 149.7, 144.2, 142.5, 140.6, 136.3,
36
37 135.0, 129.3, 128.8, 128.5, 128.2, 127.8, 127.0, 126.1, 114.7, 30.4, 22.2. HRMS–ESI (m/z):
38
39 calcd for C₂₁H₂₁ [M+H]⁺ 273.1643, found 273.1647.
40
41
42
43
44
45

46 *1,3-diphenyl-6-(cyclopropyl)fulvene 3*
47

48 To a vigorously stirred mixture of 1,3-diphenylcyclopentadiene (3.70 g, 16.9 mmol) in
49
50 absolute EtOH (30 mL) under N₂ was added cyclopropyl carboxaldehyde (1.43 g, 20.3
51
52 mmol) and pyrrolidine (1.80 g, 25.4 mmol), and the reaction mixture maintained at room
53
54
55
56
57
58
59
60

1
2
3
4
5 temperature for 24 hrs. The orange precipitate from the reaction mixture was vacuum
6
7 filtered, washed with cold absolute EtOH (3 × 10 mL), and vacuum dried to give **3** as a
8
9 bright orange, microcrystalline solid (2.38 g, 52%). ¹H NMR (500 MHz, CDCl₃) 7.71 – 7.27
10
11 (m, 10H), 7.02 (s, 1H), 6.91 (s, 1H), 5.86 (d, 1H, *J* = 10.8 Hz), 2.22 (m, 1H), 1.15, 0.77 (m,
12
13 4H). ¹³C NMR (125 MHz, CDCl₃) 149.4, 144.2, 142.8, 139.7, 136.4, 135.8, 129.3, 128.8,
14
15 128.5, 127.6, 126.9, 126.8, 126.1, 113.8, 15.0, 10.5. HRMS–ESI (*m/z*): calcd for C₂₁H₁₉
16
17 [M+H]⁺ 271.1487, found 271.1493.
18
19

20
21
22 *1,3-diphenyl-6-(2-thiophene)fulvene 5*
23

24 To a vigorously stirred mixture of 1,3-diphenylcyclopentadiene (1.25 g, 5.7 mmol) in
25
26 absolute EtOH (30 mL) under N₂ was added 2-thiophene carboxaldehyde (0.767 g, 6.8
27
28 mmol) and pyrrolidine (0.61 g, 8.6 mmol), and the reaction mixture maintained at room
29
30 temperature for 24 hrs. The red precipitate from the reaction mixture was vacuum
31
32 filtered, washed with cold absolute EtOH (3 × 10 mL), and vacuum dried to give **5** as a dark
33
34 red, microcrystalline solid (1.42 g, 80%). ¹H NMR (500 MHz, CDCl₃) 7.74 – 7.24 (m, 14H),
35
36 7.08 (m, 1H), 6.91 (s, 1H). ¹³C NMR (125 MHz, CDCl₃) 146.7, 142.2, 141.5, 140.9, 136.2,
37
38 135.4, 133.7, 131.0, 130.3, 129.5, 128.8, 128.6, 128.1, 128.0, 127.7, 127.2, 126.3, 113.8.
39
40 HRMS–ESI (*m/z*): calcd for C₂₂H₁₇S [M]⁺ 313.1051, found 313.1055.
41
42
43

44
45
46 *1,3-diphenyl-6-(2,3-dimethoxynaphthyl)fulvene 10*
47

48 To a vigorously stirred mixture of 1,3-diphenylcyclopentadiene (1.01 g, 4.6 mmol) in
49
50 absolute EtOH (30 mL) under N₂ was added 2,3-dimethoxynaphthaldehyde (1.20 g, 5.6
51
52 mmol) and pyrrolidine (0.49 g, 6.9 mmol), and the reaction mixture maintained at room
53
54
55
56
57

1
2
3
4
5 temperature for 24 hrs. The red precipitate from the reaction mixture was vacuum
6
7 filtered, washed with cold absolute EtOH (3 × 10 mL), and vacuum dried to give **10** as a
8
9 red, microcrystalline solid (1.70 g, 89%). ¹H NMR (500 MHz, CDCl₃) 7.91 – 7.21 (m, 16H),
10
11 7.03 (s, 1H), 6.43 (s, 1H), 4.01 (s, 3H), 3.82 (s, 3H). ¹³C NMR (125 MHz, CDCl₃) 152.0, 148.0,
12
13 147.6, 145.6, 140.6, 136.1, 135.1, 132.3, 131.5, 129.3, 129.0, 128.9, 128.7, 128.6, 128.0,
14
15 127.2, 127.0, 126.8, 126.2, 125.8, 125.7, 124.4, 116.7, 108.1, 61.2, 55.9. HRMS–ESI (m/z):
16
17 calcd for C₃₀H₂₅O₂ [M+H]⁺ 417.1855, found 417.1859.

18
19
20
21
22 *(4-(cyclopentylmethyl)cyclopenta-1,3-diene-1,3-diyl)dibenzene* **12b**

23
24 To a vigorously stirred mixture of 1,3-diphenylcyclopentadiene (1.00 g, 4.6 mmol) in
25
26 absolute EtOH (30 mL) under N₂ was added cyclopentyl carboxaldehyde (0.54 g, 5.5
27
28 mmol) and pyrrolidine (0.49 g, 6.9 mmol), and the reaction mixture maintained at room
29
30 temperature for 24 hrs. The yellow precipitate from the reaction mixture was vacuum
31
32 filtered, washed with cold absolute EtOH (3 × 10 mL), and vacuum dried to give **12b** as a
33
34 yellow, microcrystalline solid (0.57 g, 42%). Crystals suitable for single crystal X-ray
35
36 diffraction were obtained from DCM by slow evaporation. ¹H NMR (500 MHz, CDCl₃) 7.57
37
38 – 7.15 (m, 10 H), 7.06 (s, 1H), 6.58 (s, 1H), 3.87 (s, 2H); 2.58, 2.42, 1.84, 1.66 (m, 8H). ¹³C
39
40 NMR (125 MHz, CDCl₃) 145.7, 144.1, 142.1, 139.7, 137.1, 136.2, 131.0, 128.8, 128.4,
41
42 126.9, 126.7, 124.9, 116.9, 44.4, 36.6, 32.7, 28.6, 26.3. HRMS–ESI (m/z): calcd for C₂₃H₂₁
43
44 [M]⁺ 297.1638, found 297.1647.
45
46
47
48
49
50
51
52
53
54
55
56
57
58
59
60

Supporting Information

The supporting information is available free of charge on the ACS Publications website, <http://www.ccdc.cam.ac.uk/cont/retrieving.html> or from the CCDC, 12 Union Road, Cambridge CB21EZ, UK. Fax: +44 1223 336033. E-mail: deposit@ccdc.cam.ac.uk.

^1H and ^{13}C NMR spectra for **2**, **3**, **5**, **10**, and **12b**, text describing crystallographic details, and tables of crystallographic data for **2** (CCDC 1988531), **8** (CCDC 1988532), **11** (CCDC 1988529) and **12b** (CCDC 1988530).

Acknowledgement

We thank Professor Arnold L. Rheingold and Dr. Milan Gembicky of the University of California at San Diego (UCSD) for allowing GJB the use of state of the art X-ray diffractometers, one of which was used for the analysis of **2**, **8**, **11** and **12b** while GJB was a crystallographer in residence for a 2019 fall semester sabbatical working in the UCSD Small Molecule Crystallography Laboratory. LCB is a National Research Council (NRC) Postdoctoral Fellow funded by the Air Force Office of Scientific Research (AFOSR). AJP gratefully acknowledges the United States Air Force Institute of Technology Civilian Institutions program for graduate sponsorship. STI and GJB acknowledge financial support from the Defense Threat Reduction Agency (DTRA) and the Air Force Office of Scientific Research (AFOSR). We finally thank Dr. Thomas Lee at the University of Colorado at Boulder for high resolution mass spectrometry analysis.

References

- (1) de Gennes, P.G. A Simple Picture for Structural Glasses. *Comptes Rendus Phys.*

- 1
2
3
4
5 **2002**, 3 (9), 1263–1268.
- 6
7 (2) Sillescu, H. Heterogeneity at the Glass Transition: A Review. *J. Non. Cryst. Solids*
8
9 **1999**, 243 (2–3), 81–108.
- 10
11 (3) Mahlin, D.; Bergström, C. A. S. Early Drug Development Predictions of Glass-
12
13 Forming Ability and Physical Stability of Drugs. *Eur. J. Pharm. Sci.* **2013**, 49 (2),
14
15 323–332.
- 16
17 (4) Miyazaki, T.; Yoshioka, S.; Aso, Y.; Kawanishi, T. Crystallization Rate of Amorphous
18
19 Nifedipine Analogues Unrelated to the Glass Transition Temperature. *Int. J.*
20
21 *Pharm.* **2007**, 336 (1), 191–195.
- 22
23 (5) Baird, J. A.; Van Eerdenbrugh, B.; Taylor, L. S. A Classification System to Assess the
24
25 Crystallization Tendency of Organic Molecules from Undercooled Melts. *J. Pharm.*
26
27 *Sci.* **2010**, 99 (9), 3787–3806.
- 28
29 (6) Mahlin, D.; Ponnambalam, S.; Heidarian Höckerfelt, M.; Bergström, C. A. S.
30
31 Toward in Silico Prediction of Glass-Forming Ability from Molecular Structure
32
33 Alone: A Screening Tool in Early Drug Development. *Mol. Pharm.* **2011**, 8 (2), 498–
34
35 506.
- 36
37 (7) Zondervan, R.; Xia, T.; Van Der Meer, H.; Storm, C.; Kulzer, F.; Van Saarloos, W.;
38
39 Orrit, M. Soft Glassy Rheology of Supercooled Molecular Liquids. *Proc. Natl. Acad.*
40
41 *Sci. U. S. A.* **2008**, 105 (13), 4993–4998.
- 42
43 (8) Hogge, J. W.; Long, E. A.; Christian, M. L.; Fankhauser, A. D.; Quist, N. L.; Rice, D.
44
45 M.; Wilding, W. V.; Knotts, T. A. Melting Point, Enthalpy of Fusion, and Heat
46
47
48
49
50
51
52
53
54
55
56
57
58
59
60

- 1
2
3
4
5 Capacity Measurements of Several Polyfunctional, Industrially Important
6
7 Compounds by Differential Scanning Calorimetry. *J. Chem. Eng. Data* **2018**, *63* (7),
8
9 2500–2511.
10
11
12 (9) Kawakami, K. Crystallization Tendency of Pharmaceutical Glasses: Relevance to
13
14 Compound Properties, Impact of Formulation Process, and Implications for
15
16 Design of Amorphous Solid Dispersions. *Pharmaceutics* **2019**, *11* (5), 202.
17
18
19 (10) Gannu Praveen Kumar, B. S. K. Current Challenges in the Development and
20
21 Formulation of Amorphous Solids. *Indones. J Pharm* **2012**, *23* (2), 66–83.
22
23
24 (11) Kothari, K.; Ragoonanan, V.; Suryanarayanan, R. Influence of Molecular Mobility
25
26 on the Physical Stability of Amorphous Pharmaceuticals in the Supercooled and
27
28 Glassy States. *Mol. Pharm.* **2014**, *11* (9), 3048–3055.
29
30
31 (12) Lemmer, H. J. R.; Liebenberg, W. Preparation and Evaluation of Metastable Solid-
32
33 State Forms of Lopinavir. *Pharmazie* **2013**, *68* (5), 327–332.
34
35
36 (13) Bhattacharya, S.; Suryanarayanan, R. Local Mobility in Amorphous
37
38 Pharmaceuticals - Characterization and Implications on Stability. *J. Pharm. Sci.*
39
40 **2009**, *98* (9), 2935–2953.
41
42
43 (14) Baird, J. A.; Taylor, L. S. Evaluation of Amorphous Solid Dispersion Properties
44
45 Using Thermal Analysis Techniques. *Advanced Drug Delivery Reviews*. 2012, 396–
46
47 421.
48
49
50 (15) Wedler, W.; Demus, D.; Zschke, H.; Mohr, K.; Schäfer, W.; Weissflog, W.
51
52
53 *Vitrification in Low-Molecular-Weight Mesogenic Compounds*; 1991; Vol. 1.
54
55
56
57
58
59
60

- 1
2
3
4
5 (16) Detty, M. R.; Fleming, J. C. Novel Materials for Non-ablative Optical Recording.
6
7 *Adv. Mater.* **1994**, *6* (1), 48–51.
8
9
10 (17) Fuhrmann, T.; Salbeck, J. Functional Molecular Glasses: Building Blocks for Future
11
12 Optoelectronics. In *Advances in Photochemistry, Volume 27*; John Wiley & Sons,
13
14 Inc.: Hoboken, New Jersey, USA, 2003; 83–166.
15
16
17 (18) Braun, D.; Langendorf, R. Vitrigens. I. Synthesis and Characterization of Low
18
19 Molecular Weight Organic Glasses. *J. für Prakt. Chemie* **1999**, *341* (2), 128–137.
20
21
22 (19) Ku, K.; Joung, J. F.; Park, H.; Kim, M. G.; Park, S.; Kim, W. Fluorescent Organic
23
24 Glass with Unique Optical and Mechanical Properties. *Adv. Funct. Mater.* **2018**, *28*
25
26 (39), 1801394.
27
28
29 (20) Traskovskis, K.; Mihailovs, I.; Tokmakovs, A.; Jurgis, A.; Kokars, V.; Rutkis, M.
30
31 Triphenyl Moieties as Building Blocks for Obtaining Molecular Glasses with
32
33 Nonlinear Optical Activity. *J. Mater. Chem.* **2012**, *22* (22), 11268–11276.
34
35
36 (21) Wu, Y. C. M.; Molaire, M. F.; Weiss, D. S.; Angel, F. A.; DeBlase, C. R.; Fors, B. P.
37
38 Synthesis of Amorphous Monomeric Glass Mixtures for Organic Electronic
39
40 Applications. *J. Org. Chem.* **2015**, *80* (24), 12740–12745.
41
42
43 (22) Carlson, J. S.; Marleau, P.; Zarkesh, R. A.; Feng, P. L. Taking Advantage of Disorder:
44
45 Small-Molecule Organic Glasses for Radiation Detection and Particle
46
47 Discrimination. *J. Am. Chem. Soc.* **2017**, *139* (28), 9621–9626.
48
49
50 (23) Alig, I.; Braun, D.; Langendorf, R.; Wirth, H. O.; Voigt, M.; Wendorff, J. H. *Vitrigens:*
51
52 *Part 2. - Low Molecular Weight Organic Systems with High Glass Transition*
53
54
55
56
57
58
59
60

- 1
2
3
4
5 *Temperatures*; 1998; Vol. 8.
6
7 (24) Alig, I.; Braun, D.; Langendorf, R.; Voigt, M.; Wendorff, J. H. Simultaneous Ageing
8 and Crystallization Processes within the Glassy State of a Low Molecular Weight
9 Substance. *J. Non. Cryst. Solids* **1997**, *221* (2–3), 261–264.
10
11
12
13
14 (25) Braun, D.; Langendorf, R. Low Molecular-Weight Glassy Fulvenes. *J. für Prakt.*
15 *Chemie* **2000**, *342* (1), 80–82.
16
17
18
19 (26) Stone, K. J.; Little, R. D. An Exceptionally Simple and Efficient Method for the
20 Preparation of a Wide Variety of Fulvenes. *J. Org. Chem.* **1984**, *49* (11), 1849–
21 1853.
22
23
24
25
26 (27) Peloquin, A. J.; Stone, R. L.; Avila, S. E.; Rudico, E. R.; Horn, C. B.; Gardner, K. A.;
27 Ball, D. W.; Johnson, J. E. B.; Iacono, S. T.; Balaich, G. J. Synthesis of 1,3-Diphenyl-
28 6-Alkyl/Aryl-Substituted Fulvene Chromophores: Observation of π - π Interactions
29 in a 6-Pyrene-Substituted 1,3-Diphenylfulvene. *J. Org. Chem.* **2012**, *77* (14), 6371–
30 6376.
31
32
33
34
35
36
37
38 (28) Shurdha, E.; Repasy, B. K.; Miller, H. A.; Dees, K.; Iacono, S. T.; Ball, D. W.; Balaich,
39 G. J. Symmetrical Bis(Fulvene) Chromophores: Model Compounds for Acceptor-
40 Donor-Acceptor Dye Architectures. *RSC Adv.* **2014**, *4* (79), 41989–41992.
41
42
43
44
45
46 (29) Godman, N. P.; Adas, S. K.; Hellwig, K. M.; Ball, D. W.; Balaich, G. J.; Iacono, S. T.
47 Synthesis, Electrochemical Characterization, and Linear Free Energy Relationship
48 of 1,3-Diphenyl-6-Alkyl/Arylfulvenes. *J. Org. Chem.* **2016**, *81* (20), 9630–9638.
49
50
51
52
53 (30) Uebersax, B.; Neuenschwander, M.; Engel, P. Strukturaufklärung Eines
54
55
56
57
58
59
60

1
2
3
4
5 Dimethylfulven-Trimeren. Hinweis Auf Eine [6 + 4]-Cycloaddition von 6,
6
7 6-Dimethylfulven. *Helv. Chim. Acta* **1982**, 65 (1), 89–104.

- 8
9
10 (31) Hong, B. C.; Shr, Y. J.; Liao, J. H. Unprecedented Microwave Effects on the
11
12 Cycloaddition of Fulvenes. A New Approach to the Construction of Polycyclic Ring
13
14 Systems. *Org. Lett.* **2002**, 4 (4), 663–666.
15
16
17 (32) Adas, S. K.; Peloquin, A. J.; Iacono, S. T.; Balaich, G. J. 9-(3,5-
18
19 Dimethylbenzylidene)-8-(3,5-Dimethylphenyl)-1,3,5,7-Tetraphenyl-2,4,7,8-
20
21 Tetrahydro-4,7-Methanoazulene Acetonitrile Disolvate. *IUCrData* **2018**, 3 (4),
22
23 x180553.
24
25
26
27 (33) Peloquin, A. J.; Adas, S. K.; Iacono, S. T.; Balaich, G. J. Crystal Structures of a Series
28
29 of 6-Aryl-1,3-Diphenylfulvenes. *Acta Crystallogr. Sect. E Crystallogr. Commun.*
30
31 **2019**, 75 (6), 838–842.
32
33
34
35
36
37
38
39
40
41
42
43
44
45
46
47
48
49
50
51
52
53
54
55
56
57
58
59
60